Energy 149 (2018) 11–23

Contents lists available at ScienceDirect

Energy

journal homepage: www.elsevier.com/locate/energy

Relaxed deep learning for real-time economic generation dispatch and control with unified time scale

Linfei Yin [a], Tao Yu [a, *], Xiaoshun Zhang [a], Bo Yang [b]

[a] College of Electric Power Engineering, South China University of Technology, Guangzhou, 510640, China
[b] Faculty of Electric Power Engineering, Kunming University of Science and Technology, Kunming, 650500, China

ARTICLE INFO

Article history:
Received 12 July 2017
Received in revised form
28 January 2018
Accepted 29 January 2018
Available online 22 February 2018

2010 MSC:
00-01
99-00

Keywords:
Relaxed deep learning
Real-time economic generation dispatch and control
Unified time scale
Deep neural network

ABSTRACT

To solve the collaboration problem of multi-time scale economic dispatch and generation control in power system, i.e., long term time scale optimization, short term time scale optimization, and real-time control, a real-time economic generation dispatch and control (REG) framework, which as a unified time scale framework, is designed in this paper. With a relaxed operator employed into deep neural network (DNN), relaxed deep learning (RDL) is proposed for the REG framework, which towards an alternative to conventional generation control framework, which combines unit commitment (UC), economic dispatch (ED), automatic generation control (AGC), and generation command dispatch (GCD). Compared with 1200 combined conventional generation control algorithms in two simulations, i.e., IEEE 10-generator 39-bus New-England power system and Hainan 8-generator power grid (China), RDL obtains the optimal control performance with smaller frequency deviation, smaller area control error, smaller total cost, and smaller number of reverse regulation. Although the RDL needs a relative long computation time in the pre-training, the simulation results verify the effectiveness and feasibility of the proposed RDL for REG framework.

1. Introduction

To balance the active power between generators and load, and maintain the systemic frequency at the normal value, conventional generation control framework has been employed into multi-area power system. Generally, the conventional generation control framework is divided into thee time scales [1–3], i.e., (i) unit commitment (UC) [4], (ii) economic dispatch (ED) [5], (iii) automatic generating control (AGC) and generation command dispatch (GCD) [6–9]. However, the conventional generation control framework has several shortcomings, which are listed as follows.

(1) In a conventional generation control framework, the longer time scale means the generation commands more inaccurate. Collaboration problem between long term time scale and short term time scale could lead to reverse regulation, such as, the generation command of an ED programming is up-regulation, while the generation command of an AGC controller is down-regulation.
(2) In a conventional generation control framework, the solutions of the UC and ED programming are based on the prediction of load at next time slot, while the real-time AGC controller and GCD are based on the features of the AGC units. Consequently, the AGC controller and GCD lead to a non-optimal control from a long term view point.
(3) Generally, the objective of the long term optimization (e.g, UC) is different than that of the short term optimization (e.g., ED). Consequently, the results of these optimizations could lead to a non-optimal actions for both the long and short term.

Numerous integrated algorithms or integrated framework have been proposed to overcome the parts of these shortcomings. For instance, economic automatic generation control has been proposed considering ED combined with AGC controller [10,11]. UC and ED are combined for wind power forecasting in Ref. [12]. Moreover, ED and AGC controller have been integrated from optimization view in Ref. [13]. However, these algorithms need to be improved for all of the above shortcomings.

* Corresponding author.
E-mail address: taoyu1@scut.edu.cn (T. Yu).

https://doi.org/10.1016/j.energy.2018.01.165
0360-5442/

To avoid these problems, this paper proposed a real-time economic generation dispatch and control (REG) framework, which towards an alternative to the conventional generation control framework. Besides, this paper proposed relaxed deep learning (RDL) algorithm for this REG framework. The controller for REG framework is a unified time scale controller for generation dispatch and control in power system, which is set to be 4 s usually. RDL is based on deep neural network (DNN) and relaxed operator, which is a constrained operator for AGC units. DNN in the field of deep learning becomes more and more popular, especially for the game of Go [14]. For example, deep reinforcement learning (DRL) has been applied to solve the problem of high-dimensional sensory inputs [15]. Active classification of electrocardiogram signals can been learned by deep learning [16]. Deep convolutional nets have brought breakthroughs in processing images, video, speech and audio [17]. To compare with the artificial neural network and DNN, relaxed artificial neural network (RANN) is designed in this paper, which is based on artificial neural network and relaxed operator. Features of RDL can be summarized as follows,

(1) As a unified time scale controller, RDL can avoid the collaboration problem of multiple time scales at long term view point.
(2) With the multiple output ability of DNN in RDL, RDL can simultaneously output multiple generation commands for AGC units.
(3) With the learning ability of deep learning, RDL can predict the state of dynamic system.
(4) With the relaxed operator, RDL, which has the unified control objective, can commit the constraints of generating units.

The remaining of this paper is organized as follows. The model of a conventional generation control framework is developed in Section 2. Section 3 describes basic principle of RDL algorithm and REG framework. Simulation results are presented in Section 4. Section 5 discusses the features of the RDL based REG controller. Section 6 briefly concludes the paper.

2. Model of conventional generation control framework

A conventional generation control framework contains four process, i.e., UC, ED, AGC, and GCD (Fig. 1). The UC programs the start-up or shut-down states of units, and active power production level at a long period, such as one day [18]. Then, ED reprograms generation commands for all the start-up units at a short period, such as 15 min. Lastly, AGC controller and GCD re-reprograms the real-time generation commands for all the AGC units.

2.1. Model of unit commitment

UC programming aims to find an optimal schedule for units start-up or shut-down and a production level over a given period of time. Consequently, UC problem is a stochastic mixed 0-1 integer programming problem, which can be solved by programming or optimization algorithm.

The optimization objective of UC problem is minimize the total cost of generation,

$$\min \sum_{t=1}^{T} \sum_{j=1}^{J_i} [F_j(P_{j,t}) u_{j,t} + SU_{j,t}(1 - u_{j,t-1}) u_{j,t}] \tag{1}$$

where T is the number of time slots over the given period of time; J_i is the number of generating units in the i-th area; $u_{j,t}$ is the state of the j-th generating unit at the t-th time slot, while $u_{j,t} = 1$ for start-up state and $u_{j,t} = 0$ for shut-down state. The total cost of generation includes the fuel cost of the j-th generating $F_j(P_{j,t})$ and start-up cost $SU_{j,t}$:

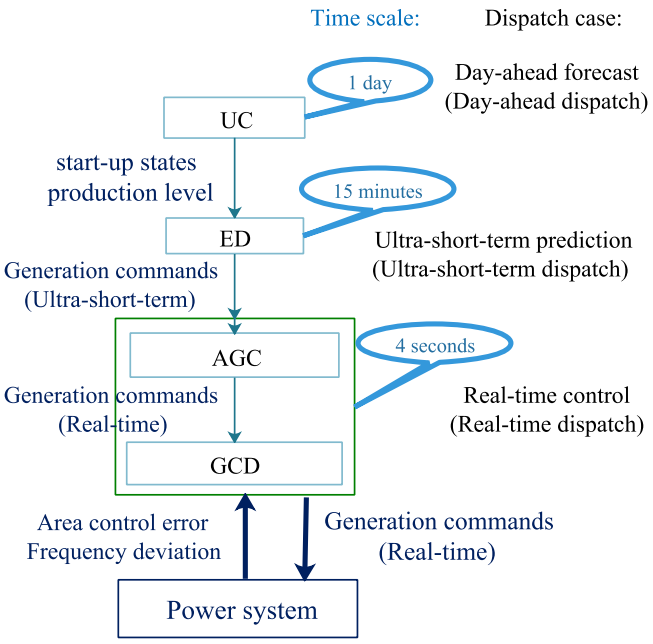

Fig. 1. Model of conventional generation control framework.

$$F_j(P_{j,t}) = a_j + b_j P_{j,t} + c_j P_{j,t}^2 \tag{2}$$

$$SU_{j,t} = \begin{cases} SU_{H,j}, \text{if } T_j^{\text{min-down}} \le T_{j,t}^{\text{up}} \le T_j^{\text{min-down}} + T_j^{\text{cold}} \\ SU_{C,j}, \text{if } T_{j,t}^{\text{down}} > T_j^{\text{min-down}} + T_j^{\text{cold}} \end{cases} \tag{3}$$

where $P_{j,t}$ is the active power of the j-th generating unit at the t-th time slot; a_j, b_j and c_j are the constant factor, linear factor, and quadratic factor of the generation cost, respectively; $T_{j,t}^{\text{up}}$ and $T_{j,t}^{\text{down}}$ are the accumulate time slots of start-up state and shut-down state for the j-th generating unit at the t-th time slot, respectively; $T_j^{\text{min-down}}$ is the minimized continuous shut-down time slot of the j-th generating unit; T_j^{cold} is the time slots of the j-th generating unit for cold start-up, which start from entirely shut-down state; $SU_{H,j}$ and $SU_{C,j}$ are the j-th generating unit cost of heat start-up and cold start-up, respectively.

Constraints of UC problem contain active power balance constraint, spinning reserve constraint, active power limit constraint, generation rate constraint,

$$\begin{cases} \sum_{j=1}^{J_i} P_{j,t} u_{j,t} = PD_{i,t} \\ \sum_{j=1}^{J_i} P_j^{\max} u_{j,t} \ge PD_{i,t} + SR_{i,t} \\ u_{j,t} P_j^{\min} \le P_{j,t} \le u_{j,t} P_j^{\max} \\ 0 \le P_{j,t} - P_{j,(t-1)} \le P_j^{\text{up}} \\ 0 \le P_{j,t} - P_{j,(t-1)} \le P_j^{\text{down}} \end{cases} \tag{4}$$

where $PD_{i,t}$ is the total of system load at the t-th time slot in the i-th area; $P_j^{\min}$ and $P_j^{\max}$ are the minimum and the maximum active

power of the j-th generating unit in the i-th area, respectively; $SR_{i,t}$ is the needed systemic spinning reserve at the t-th time slot in the i-th area; P_j^{up} and P_j^{down} are the maximum amplitude of the j-th generating unit for up-regulation and down-regulation, respectively; $T_j^{\text{min-up}}$ is the minimized continuous start-up time slot of the j-th generating unit. Constraint of $u_{j,t}$ can be calculated as,

$$u_{j,t} = \begin{cases} 0, & \text{if } u_{j,(t-1)} = 0 \ \& \ u_{j,t}^* = 0 \\ 0, & \text{if } u_{j,(t-1)} = 0 \ \& \ u_{j,t}^* = 1 \& \ 1 \le T_{j,(t-1)}^{\text{down}} < T_j^{\text{min-down}} \\ 1, & \text{if } u_{j,(t-1)} = 0 \ \& \ u_{j,t}^* = 1 \ \& \ T_{j,(t-1)}^{\text{down}} \ge T_j^{\text{min-down}} \\ 1, & \text{if } u_{j,(t-1)} = 1 \ \& \ u_{j,t}^* = 0 \ \& \ 1 \le T_{j,(t-1)}^{\text{up}} < T_j^{\text{min-up}} \\ 0, & \text{if } u_{j,(t-1)} = 1 \ \& \ u_{j,t}^* = 0 \ \& \ T_{j,(t-1)}^{\text{up}} \ge T_j^{\text{min-up}} \\ 1, & \text{if } u_{j,(t-1)} = 1 \ \& \ u_{j,t}^* = 1 \end{cases} \tag{5}$$

where $u_{j,1}^*$ is the temporary state of the j-th generating unit at the t-th time slot, and it is programmed by the UC; $u_{j,(t-1)}$ is the state of the j-th generating unit at the $(t-1)$-th time slot, and the initial value $u_{j,1}^*$ will not be reset; the state of the j-th generating unit at the t-th time slot should be reset to start-up state when the time of continuous start-up state $T_{j,(t-1)}^{\text{up}}$ is less then the minimized continuous start-up time slot $T_j^{\text{min-up}}$, i.e., $u_{j,t} = 1$; the state of the j-th generating unit at the t-th time slot should be reset to shut-down state when the time of continuous shut-down state $T_{j,(t-1)}^{\text{down}}$ is less then the minimized continuous shut-down time slot $T_j^{\text{min-down}}$, i.e., $u_{j,t} = 0$.

2.2. Model of economic dispatch

ED reprograms generation commands with economic way, which can be solved by optimization algorithm. The ED objective mainly contains three objectives, i.e., economic objective, carbon emission reduction, and network losses. The economic objective aims to minimize the total generation cost of the system,

$$F_{\text{total}}^{\text{e}} = \sum_{j=1}^{J_i} F_j^{\text{e}}(P_j) = \sum_{j=1}^{J_i} \left(c_j P_j^2 + b_j P_j + a_j \right) \tag{6}$$

where $F_j^{\text{e}}(P_j)$ is the generation cost of the j-th generating unit; P_j is the active power of the j-th generating unit.

The carbon emission reduction aims to reduce the carbon dioxide (CO^2) emissions come from combustion of fossil fuels, principally coal, oil, etc.

$$F_{\text{total}}^{\text{c}} = \sum_{j=1}^{J_i} F_j^{\text{c}}(P_j) = \sum_{j=1}^{J_i} \left(\alpha_j P_j^2 + \beta_j P_j + \gamma_j \right) \tag{7}$$

where γ_j, β_j and α_j are the constant factor, linear factor, and quadratic factor of the j-th generating unit for carbon emission, respectively; $F_j^{\text{c}}(P_j)$ is the carbon emission of the j-th generating unit.

The network losses can be given by Kron's approximate loss formula [19], as follows:

$$F_{\text{total}}^{\text{K}} = K_{\mathbf{Lo}} + \sum_{j=1}^{J_i} B_{j0} P_j + \sum_{i=1}^{J_i} \sum_{j=1}^{J_j} B_{ij} P_i P_j \tag{8}$$

where $K_{\mathbf{Lo}}$, B_{j0}, and B_{ij} are loss formula coefficients.

An alternatively more accurate representation can be given as [19]:

$$F_{\text{total}}^{\text{K}} = \sum_{j=1}^{J_i} P_j - PD_i \tag{9}$$

where PD_i is the total systemic load in the i-th area.

Considering these three objectives with a line weight, the model of ED can be described as,

$$\min F_{\text{total}} = \omega_{\text{e}} F_{\text{total}}^{\text{e}} + \omega_{\text{c}} F_{\text{total}}^{\text{c}} + \omega_{\text{K}} F_{\text{total}}^{\text{K}}$$
$$s.t. \begin{cases} P_j^{\min} \le P_j \le P_j^{\max} \\ P_{j,t} - P_{j,t-1} \le P_j^{\text{up}} \\ P_{j,t-1} - P_{j,t} \le P_j^{\text{down}} \\ 0 < \omega_{\text{e}}, \omega_{\text{c}}, \omega_{\text{K}} < 1 \\ \omega_{\text{e}} + \omega_{\text{c}} + \omega_{\text{K}} = 1 \end{cases} \tag{10}$$

where ω_{e}, ω_{c}, and ω_{K} are the weights of economic objective, carbon emission reduction, and network losses, respectively.

2.3. Model of automatic generation control

As a conventional real-time control system, an AGC model of a two-area power system is illustrated in Fig. 2. The inputs of the AGC controller are the frequency deviation Δf_i and the area control error (ACE) e_i of the i-th area, and the output of the AGC controller is generation command ΔP_i for the i-th area. The control period of AGC model is second grade, while usually is set to be 4 s or 8 s.

2.4. Model of generation command dispatch

Input of GCD is generation command, which obtained by AGC controller, and outputs of GCD are generation commands $\Delta P_{i,j}$ for all the AGC units in the i-th area. Then, the actual generation command $P_{i,j}^{\text{actual}}$ of the j-th AGC unit in the i-th area is the sum of the generation commands from both ED and GCD, i.e., $P_{i,j}^{\text{actual}} = P_{i,j} + \Delta P_{i,j}$. In practice, the objective of GCD is the economic objective, as Eq. (6).

3. Relaxed deep learning

3.1. Conventional control algorithms and optimization algorithms

Frequency control contains three regulation processes, i.e., primary frequency regulation, secondary frequency regulation, tertiary frequency regulation. Since primary frequency regulation or primary frequency control, which regulated systemic frequency by generating unit in short period, is a difference control, secondary frequency regulation and tertiary frequency regulation have been designed to balance the active power between generators and load. Secondary frequency regulation and tertiary frequency regulation contain the combined algorithms, i.e., combined UC, ED, AGC, and GCD. Control algorithm for the AGC controller, while optimization algorithms for UC, ED and GCD. Consequently, a conventional generation control algorithm is the combined algorithm with 'optimization algorithm + optimization algorithm + control algorithm + optimization algorithm'.

Numerous optimization algorithms can be applied to UC, ED, and GCD. For example, genetic algorithm, particle swarm optimization [20]. Moreover, simulated annealing arithmetic has been employed to unit commitment [21]. Multi-verse optimizer has

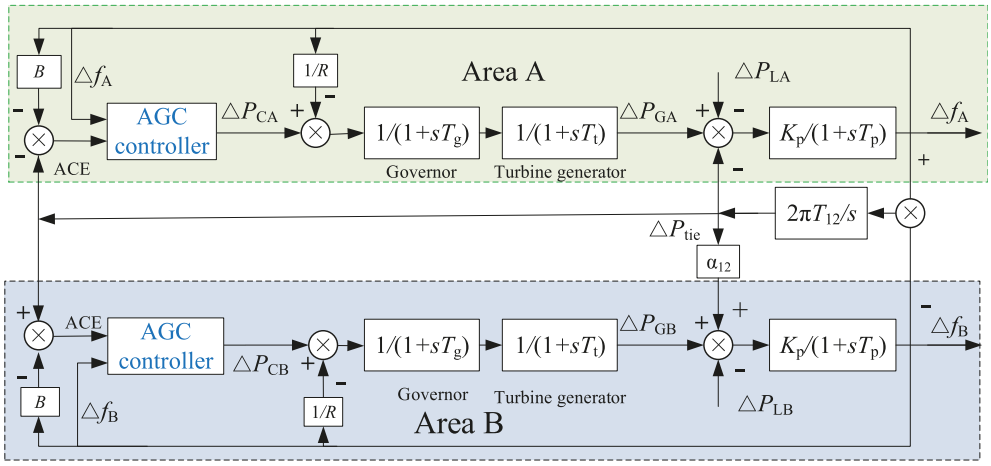

Fig. 2. AGC model of two-area power system.

been proposed and employed into training feedforward neural networks [22,23]. Grey wolf optimizer has been proposed, applied to training multi-layer perception and developed for maximum power point tracking of double-fed induction generator based wind turbine [24–26]. In practice, UC and ED are constrained optimization problems. When equality constraint is considered, the last variable of the optimizable variables is calculated by the equality equation. Then, the last variable is checked by inequality equations. The fitness value is calculated by fitness function if the last variable pass the check. In contrast, the fitness value is set to be positive infinity $(+\infty)$ if the last variable does not pass the check. Various control algorithms can be employed in AGC controller. Such as, the traditional proportional-integral-differential (PID), fuzzy logic control and fuzzy PID have been studied for load frequency control [27,28]. An optimal algorithm tuned sliding mode controller has been proposed for AGC controller of interconnected multi-area power system under deregulated environment [29]. A two-layer active disturbance rejection control method with the compensation of equivalent input disturbances has been proposed to improve the dynamic performance of load frequency control [30]. A two degree of freedom fractional order PID controller has been employed in AGC controller of power system [31]. Reinforcement learning algorithms also have been applied for AGC controller of large-scale power systems, such as, Q learning [32,33], Q(λ) learning [34] and R(λ) learning [35].

In the i-th area: UC programs start-up states $u_{i,j,t}$ and production level $P_{i,j,t}$ with the load prediction $PD_{i,t}$ of next day, where t is hour time slot of one day, i.e., $t = \{1, 2, \ldots, 24\}$; ED programs active power $P_{i,j}$ for next 15 min with ultra-short-term load prediction PD_i in next 15 min; AGC controller calculates the total generation command ΔP_i for the i-th area; GCD dispatchs the total generation command ΔP_i to each AGC unit $\Delta P_{i,j}$ in the i-th area. Table 1 shows the relationship between these three regulation processes and the conventional generation control framework.

3.2. Relaxed deep learning, and real-time economic generation dispatch and control

The proposed RDL can be designed as a REG controller, which towards an alternative to the combined algorithm, i.e., UC, ED, AGC and GCD. Therefore, inputs of the REG controller are frequency deviation Δf_i and area control error e_i, while outputs of the REG controller are generation commands $\Delta P_{i,j}$ for AGC units.

Two DNNs are designed into the proposed RDL (see Fig. 3), i.e., 'DNN1' and 'DNN2'. 'DNN1' is designed for the prediction of next states, which are frequency deviations $\Delta F'_{i,(t+1)}$ in the REG framework. Therefore, Δf_i and e_i are the inputs of 'DNN1'. Moreover, the initial actions set A is generated as,

$$A = \begin{bmatrix} a_{1,1} & a_{1,2} & \cdots & a_{1,k} \\ a_{2,1} & a_{2,2} & \cdots & a_{2,k} \\ \vdots & \vdots & \ddots & \vdots \\ a_{J_i,1} & a_{J_i,2} & \cdots & a_{J_i,k} \end{bmatrix} \tag{11}$$

where A has k columns, and each column is a generation command vector of actions for AGC units. Prediction of next state has k columns, while each column is the prediction for each action vector. Therefore, $\Delta F'_{i,(t+1)}$ has k columns for prediction of all k columns actions. 'DNN2' is developed for the dispatch of generation command $\Delta P_{i,j}$ to each AGC unit. Both inputs and outputs of 'DNN1' and

Table 1
Relationship between regulation processes and conventional generation control framework.

Con.[a]	Regulation	Algorithm	Time slot	Inputs	Outputs	Equations
UC	Ter.[b]	OA[d]	24 (h)	$PD_{i,t}$	$u_{i,j,t}$, $P_{j,t}$	Eqs. (1)–(5)
ED	Sec.[c]	OA[d]	15 (m)	PD_i	$P_{i,j}$	Eq. (6)–(10)
AGC	Sec.[c]	CA[e]	4 (s)	e_i, Δf_i	ΔP_i	Appendix B
GCD	Sec.[c]	OA[d]	4 (s)	ΔP_i	$\Delta P_{i,j}$	Appendix B, Eq. (6)
REG	Ter.[b] and Sec.[c]	CA[e]	4 (s)	Δf_i,e_i,A	$\Delta P_{i,j}$	Eq. (11)–(19)

[a] Con. = Conventional generation control or REG controller.
[b] Ter. = Tertiary frequency regulation.
[c] Sec. = Secondary frequency regulation.
[d] OA = Optimization algorithm.
[e] CA = Control algorithm.

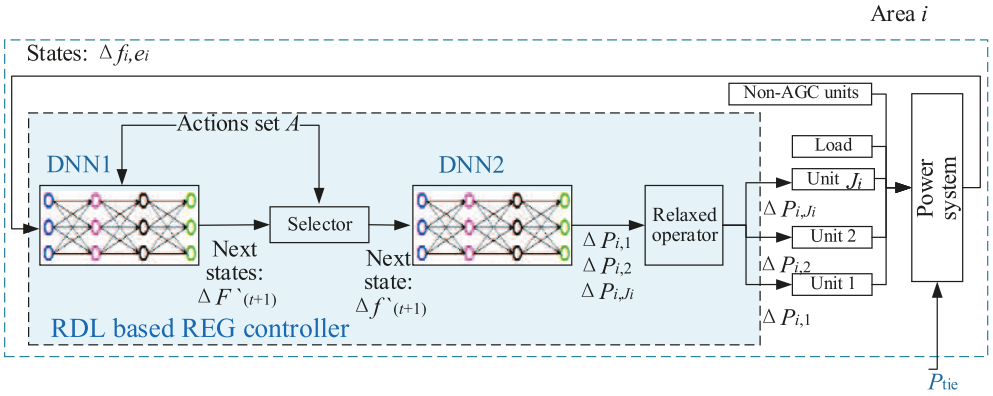

Fig. 3. Procedures of RDL based REG controller.

Table 2
Inputs and outputs of 'DNN1' and 'DNN2'.

	'DNN1'	'DNN2'
Inputs	$\Delta f_i, e_i, A$	$\Delta F'_{i,(t+1)}$
Outputs	$\Delta f'_{i,(t+1)}$	$\Delta P_{i,j}$

'DNN2' are tabulated in Table 2.

'Selector' in Fig. 3 is designed to select the optimal next state (smallest $\left|\Delta f'_{i,(t+1)}\right|$) in the next states ($\Delta F'_{i,(t+1)}$). 'Relaxed operator' is an operator to constrain the outputs of 'DNN2. Consequently, the constraint for 'Relaxed operator' can be calculated as,

$$\Delta P_{i,j} = \frac{r\left(\Delta P_{i,j} u'_{j,t}\right) \sum_{k=1}^{J_i} \left(\Delta P_{i,k}\right)}{\sum_{k=1}^{J_i} \left(r\left(\Delta P_{i,k} u'_{j,t}\right)\right)} \tag{12}$$

where $r(\Delta P_{i,j} u'_{j,t})$ is the constraint function, which can be described as,

$$\max\left\{P_{j,(t-1)} - P_j^{\text{down}}, u'_{j,t} P_j^{\min}\right\} \le \Delta P_{i,j} u'_{j,t} \le \min\left\{P_{j,(t-1)} + P_j^{\text{up}}, u'_{j,t} P_j^{\max}\right\} \tag{13}$$

where $u'_{j,t}$ is the temporary start-up state, which can be calculated as,

$$u'_{j,t} = \begin{cases} 1, & [\Delta P_{i,j}] > 0 \text{ or } 1 \le T^{\text{up}}_{j,(t-1)} < T_j^{\text{min-up}} \\ 0, & [\Delta P_{i,j}] = 0 \text{ or } 1 \le T^{\text{down}}_{j,(t-1)} < T_j^{\text{min-down}} \end{cases} \tag{14}$$

Both 'DNN1' and 'DNN2' are based on restricted Boltzmann machines. Generally, greedy-wise method is applied during the training of the two DNNs. The energy of a restricted Boltzmann machine system is defined as

$$E(\mathbf{v}, \mathbf{k}|\mathbf{q}) = -\sum_{m=1}^{M} \varphi_m v_m - \sum_{n=1}^{N} \mu_n k_n - \sum_{n=1}^{N} \sum_{m=1}^{M} v_m W_{mn} k_n \tag{15}$$

where W_{mn} is the weight in the restricted Boltzmann machine. v_m and k_n are the m-th visible unit and the n-th hidden unit, respectively. φ_m and μ_n are the offset of the m-th visible unit and the n-th hidden unit, respectively. M and N are the number of visible units and hidden units, respectively.

In particular, joint probability distribution is calculated by

$$P(\mathbf{v}, \mathbf{k}|\mathbf{q}) = \frac{e^{-E(\mathbf{v},\mathbf{k}|\mathbf{q})}}{Z(\mathbf{q})} \tag{16}$$

where $Z(\mathbf{q}) = \sum_{\mathbf{v},\mathbf{k}} e^{-E(\mathbf{v},\mathbf{k}|\mathbf{q})}$ is a normalization function. The activation probability of hidden unit is written as

$$P(k_n = 1|\mathbf{v}, \mathbf{q}) = \sigma\left(\mu_n + \sum_m v_m W_{mn}\right) \tag{17}$$

where $\sigma(\bullet)$ is defined as a sigmoid activation function $\sigma(x) = \frac{1}{1+e^{-x}}$. Activation probability of visible unit is

$$P(v_m = 1|\mathbf{k}, \mathbf{q}) = \sigma\left(\varphi_m + \sum_n k_n W_{mn}\right) \tag{18}$$

The probability of action is chosen as

$$a = \begin{cases} r_p \ln(2p), p < 0.5 \\ -r_p \ln[2(1-p)], p \ge 0.5 \end{cases} \tag{19}$$

where p is the updated probability of action a, k_p is the probability coefficient.

The 'Relaxed operator' can output generation commands for all the AGC units in the i-th area (Fig. 4).

4. Case studies

All the Simulation model and programs of this paper are developed on an Intel Core 8 Duo processor of 2.40 GHz and 8 GB RAM computer in the MATLAB version 9.1 (R2016b).

Table 3 shows all the algorithms, which are employed in the following two simulations.

The configured simulation time of each combined algorithm or REG controller is set to be 1 day. The total of 5 UC algorithms, 5 ED algorithms, 8 AGC algorithms, 6 GCD algorithms, and 2 REG algorithms are simulated (Table 3). Since these algorithms are employed in two simulations, the total configured simulation time of the two simulations is 6.586 years or $2 \times (5 \times 5 \times 8 \times 6 + 2)$ days. The parameters of these conventional generation control algorithms are presented in Appendix B.

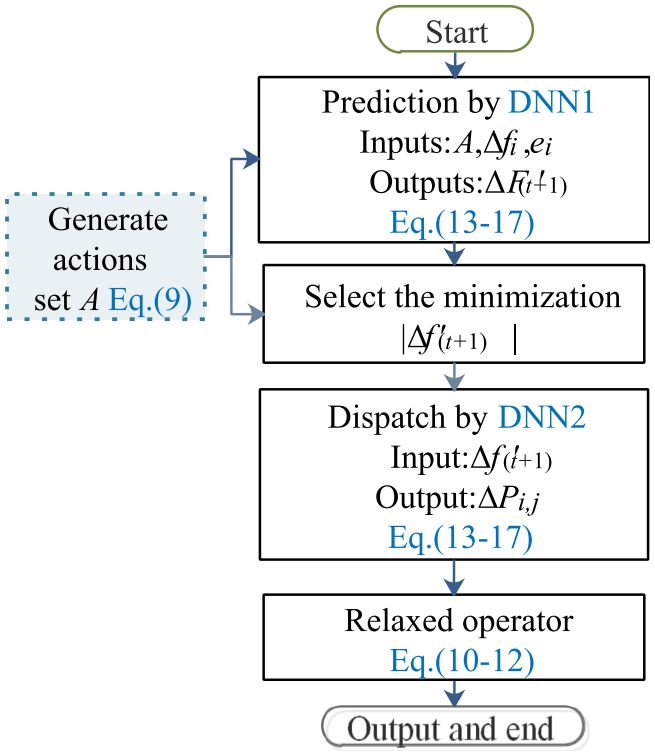

Fig. 4. Steps of the RDL based REG controller.

4.1. IEEE New-England power system

IEEE New-England power system is well known as 10-generator 39-bus power system. In this simulation, New-England system (Fig. 5) is divided into 3 areas, i.e., area 1, area 2, area 3. New-England power system has 10 generators, i.e., generator {30, 37, 39} for area 1, generator {31, 32, 33, 34, 35} for area 2, generator {36, 38} for area 3. Table 4 shows parameters of these generators. Table 5 shows the parameters of the UC problem. Besides, three new and renewable energy sources have been employed in this simulation, i.e., wind power, photovoltaic power (PV), electric vehicle (EV) (Fig. 6). The EV curve is a superposition of five different car-user profiles, i.e., (1) People going to work with a possibility to charge their car at work; (2) People going to work with a possibility to charge their car at work but with a longer ride; (3) People going to work with no possibility to charge their car at work; (4) People staying at home; (5) People working on a night shift.

In this simulation, the configured control period of generation control is set to be 4 s, i.e., the controller will provide generation commands at every control period, such as, 0 s, 4 s, 8 s, 12 s, etc. The REG controller is calculated at each control period, i.e., 0 s, 4 s, 8 s, 12 s, etc. For the combined algorithms: UC is programmed at the time of 0 s (00:00:00 a.m. everyday), i.e., 0 s, 86,400 s, 172,800 s, 259,200 s, etc.; ED is optimized at each 15 min, i.e., 0 s, 900 s, 1800 s, 2700 s, etc.; AGC controller and GCD are calculated at each control period, i.e., 0 s, 4 s, 8 s, 12 s, etc. Each artificial neural network in RANN has 40 hidden units. Each DNN in RDL has 4 layers, which 20 hidden units in each layer. The pre-training time of RANN and RDL are 6.06 and 15.55 h, respectively. Two objectives (Economic objective and carbon emission reduction with $\omega_e = 0.5$ and $\omega_c = 0.5$, see Table 6 and Fig. 7) and three objectives (All the objectives of ED with $\omega_e = 1/3$, $\omega_c = 1/3$, and $\omega_K = 1/3$, see Table 7) are considered in this case.

Fig. 7, Tables 6 and 7 demonstrate that:

(1) Compared with the combined algorithms and RANN, the proposed RDL obtains the optimal control performance (smaller frequency deviation, smaller area control error, smaller total cost, and smaller number of reverse regulation) for the multi-area power system.
(2) The power system can be effective predicted by 'DNN1' in RDL exactly.
(3) The REG controller can replace the combined algorithms for economic dispatch and generation control of multi-area power system.
(4) Since RDL can simultaneously output multiple generation commands for AGC units, RDL can be employed in REG controller.

4.2. Hainan power grid

This simulation is based on the model of Hainan (China) power gird at the year of 2015. Hainan power grid (Fig. 8) has 4 Non-AGC units and 8 AGC units, which means that Hainan power grid is a multi-output system. Hainan power grid ties line with Guangdong power grid, which is one province of the China Southern Power Grid. And the China Southern Power Grid has five provinces, i.e., Hainan power grid, Guangdong power grid, Guangxi Power, Yunnan power grid, Guizhou power grid. In this simulation, the combined algorithms and REG controllers are employed in the Hainan power gird, which is one area of a large-scale multi-area interconnected power system. Besides, in the simulation, the configuration of RDL and RANN are the same with that of in the above IEEE New-England power system. The pre-training time of RANN and RDL are 2.27 and 4.82 h in the simulation, respectively. Two objectives (Economic objective and carbon emission reduction with $\omega_e = 0.5$, and $\omega_c = 0.5$, see Table 8 and Fig. 9) and three objectives (All the objectives of ED with $\omega_e = 1/3$, $\omega_c = 1/3$, and $\omega_K = 1/3$, see Table 9) are considered in this case.

Table 3
Algorithms for two simulations.

UC and ED	AGC	GCD
Simulated annealing arithmetic	PID	Simulated annealing arithmetic
Multi-verse optimizer	Sliding mode controller	Multi-verse optimizer
Genetic algorithm	Active disturbance rejection control	Genetic algorithm
Grey wolf optimizer	Fractional order PID	Grey wolf optimizer
Particle swarm optimization	Fuzzy logic control	Particle swarm optimization
	Q learning	Fixed proportion
	Q(λ) learning	
	R(λ) learning	
RANN		
RDL		

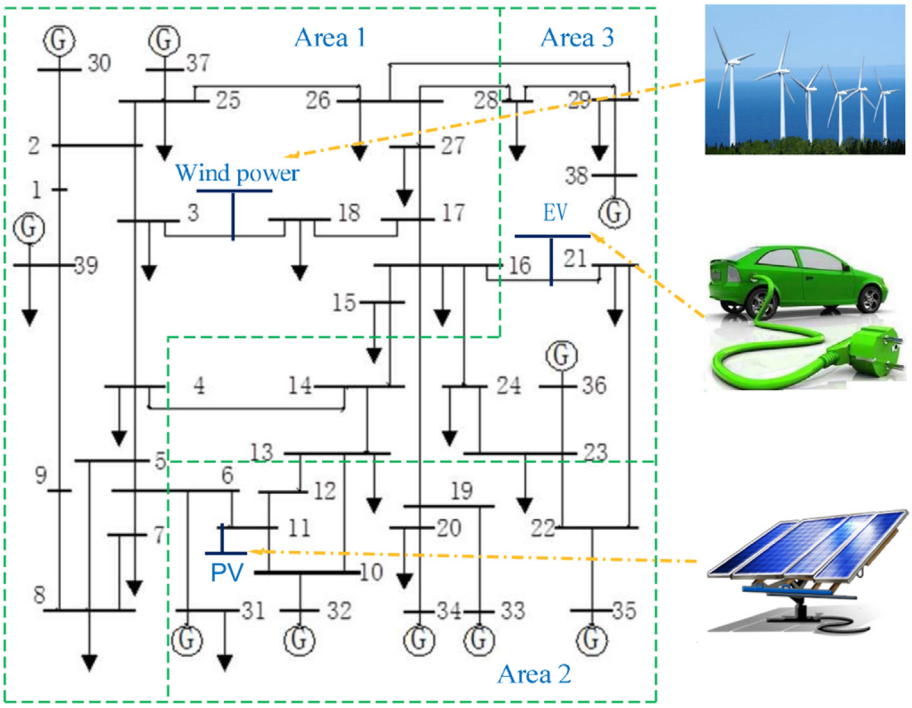

Fig. 5. Structure of New-England power system (10-generator, 39-bus).

Table 4
Parameters of 10 generators.

Generator	30	37	39	31	32	33	34	35	36	38
Area	1	1	1	2	2	2	2	2	3	3
T_j^{min-up}(h)	8	8	5	5	6	3	3	1	1	1
$T_j^{min-down}$(h)	8	8	5	5	6	3	3	1	1	1
P_j^{up}(MW/h)	200	200	200	200	200	200	200	200	200	200
P_j^{max}(MW)	455	455	130	130	162	80	85	55	55	55
P_j^{min}(MW)	150	150	20	20	25	20	25	10	10	10
a_j	1000	970	700	680	450	370	480	660	665	670
b_j	16.19	17.26	16.6	16.5	19.7	22.26	27.74	25.92	27.27	27.79
c_j	0.00048	0.00031	0.002	0.00211	0.00398	0.00712	0.00079	0.00413	0.00222	0.00173
$SU_{H,j}$(t/(MW·h))	4500	5000	550	560	900	170	260	30	30	30
$SU_{C,j}$(t/(MW h))	9000	10,000	1100	1120	1800	340	520	60	60	60
T_j^{cold}(h)	5	5	4	4	4	2	2	0	0	0
α_j	3.375	1.125	1.689	1.576	1.17	1.576	1.576	0.674	0.63	0.574
β_j	1800	600	897	837	624	837	837	362	404	290
γ_j	56,250	18,770	28,170	26,290	19,530	26,290	26,290	11,060	13,800	10,540

Table 5
Parameters of unit commitment.

t(h)	1	2	3	4	5	6	7	8	9	10	11	12
$PD_{i,t}$ (WM)	700	750	850	950	1000	1100	1150	1200	1300	1400	1450	1500
$SR_{i,t}$(WM)	70	75	85	95	100	110	115	120	130	140	145	150
t(h)	13	14	15	16	17	18	19	20	21	22	23	24
$PD_{i,t}$ (WM)	1400	1300	1200	1050	1000	1100	1200	1400	1300	1100	900	800
$SR_{i,t}$(WM)	140	130	120	105	100	110	120	140	130	110	90	80

Fig. 9, Tables 8 and 9 highlight that,

(1) The RDL based REG controller can obtain the optimal control performance in the engineering simulation.

(2) The proposed REG framework can be an alternative to the conventional generation control framework, which combines economic dispatch and generation control in multi-area power system.

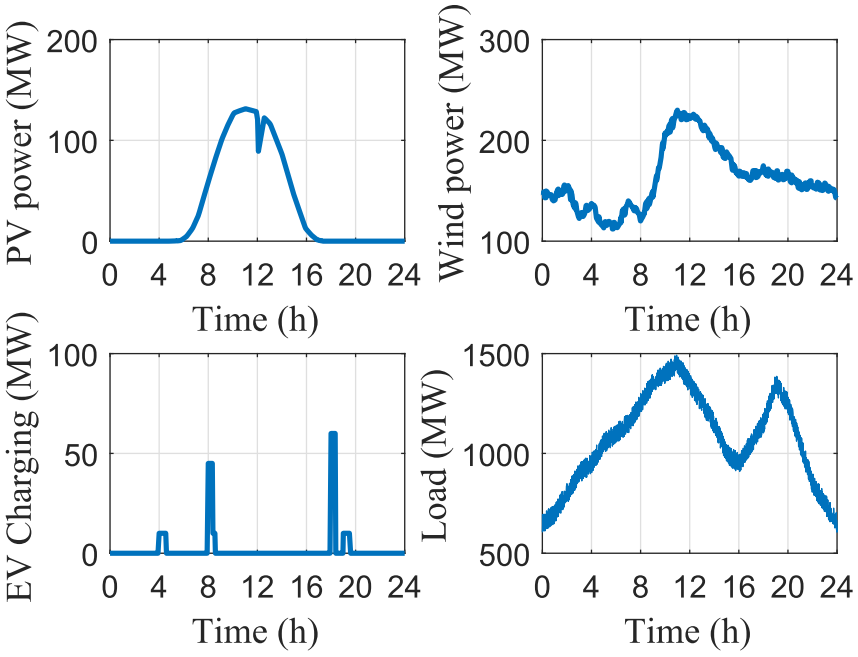

Fig. 6. Curves of PV, wind power, EV, load.

Table 6
Statistic of simulation results (New-England power system, two objectives).

Algorithm	$\|\Delta f\|$(Hz)	ACE(MW)	Total cost($)	Tim.[a] (s)	Num.[b]
RDL	0.08575	618.3755	4,121,606,894.92	0.038839	19,000
RANN	0.58476	2631.5314	5,628,016,257.08	0.04765	47,010
UC + ED + AGC + GCD	0.46647	2133.3423	4,737,044,709.77	883.1527	47,025

[a] Tim. = Calculation time.
[b] Num. = Number of reverse regulations.

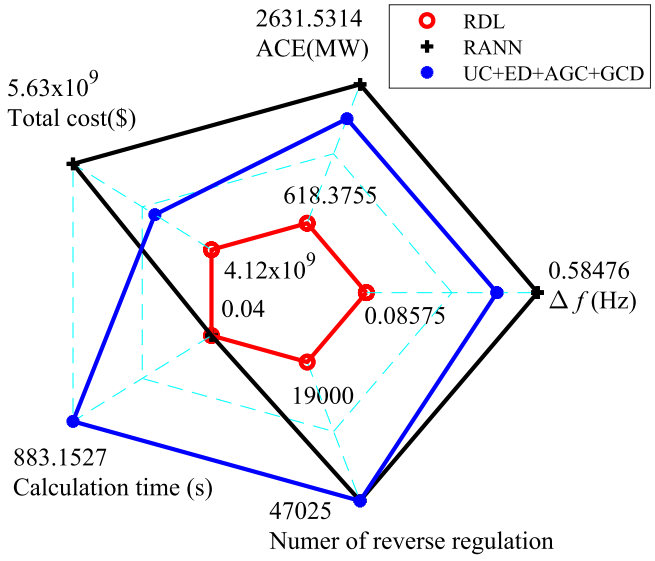

Fig. 7. Simulation results of New-England power system (frequency deviation, ACE, cost, calculation time, number of regulation).

4.3. IEEE 118-bus power system

To verify the effectiveness and feasibility of the proposed technique in a large-scale interconnected power system, the IEEE 118-bus power system with 3 control areas, 54 generators, and 186 branches (see Fig. 10) is used for testing. For this system, the number of hidden units for each artificial neural network in RANN is set to be 90, as well as for that of each DNN in RDL with 4 layers.

As shown in Fig. 11, it can be found that:

(1) Even for the large-scale power system, the RDL based REG controller can still obtain the most optimal control performance.
(2) After the RDL based REG controller has been trained, the proposed REG framework can be applied to the conventional generation control framework in a large-scale interconnected power system.
(3) The restricted Boltzmann machine of DNN can predict the next states of the power system with the different actions, then the 'Selector' of RDL will select the most eligible action for the controller.

5. Discussions

Simulation results verified that the RDL based REG controller can avoid the collaboration problem between the generation dispatch of multiple time scales. Both the frequency deviations and costs can be reduced due to three major reasons, including: (i) the RDL based REG controller is a unified time scale controller, which has no collaboration problem between the generation dispatches of multiple time scales; (ii) the DNNs of the RDL can not only predict

Table 7
Statistic of simulation results (New-England power system, three objectives).

Algorithm	$\|\Delta f\|$(Hz)	ACE(MW)	Total cost($)	Tim.[a] (s)	Num.[b]
RDL	0.1775	952.7137	1,006,513,566.21	0.051786	10,288
RANN	0.58989	2631.0365	1,712,153,075.89	0.04122	12,356
UC + ED + AGC + GCD	0.43006	1969.9137	1,997,109,548.61	930.168	25,054

[a] Tim. = Calculation time.
[b] Num. = Number of reverse regulations.

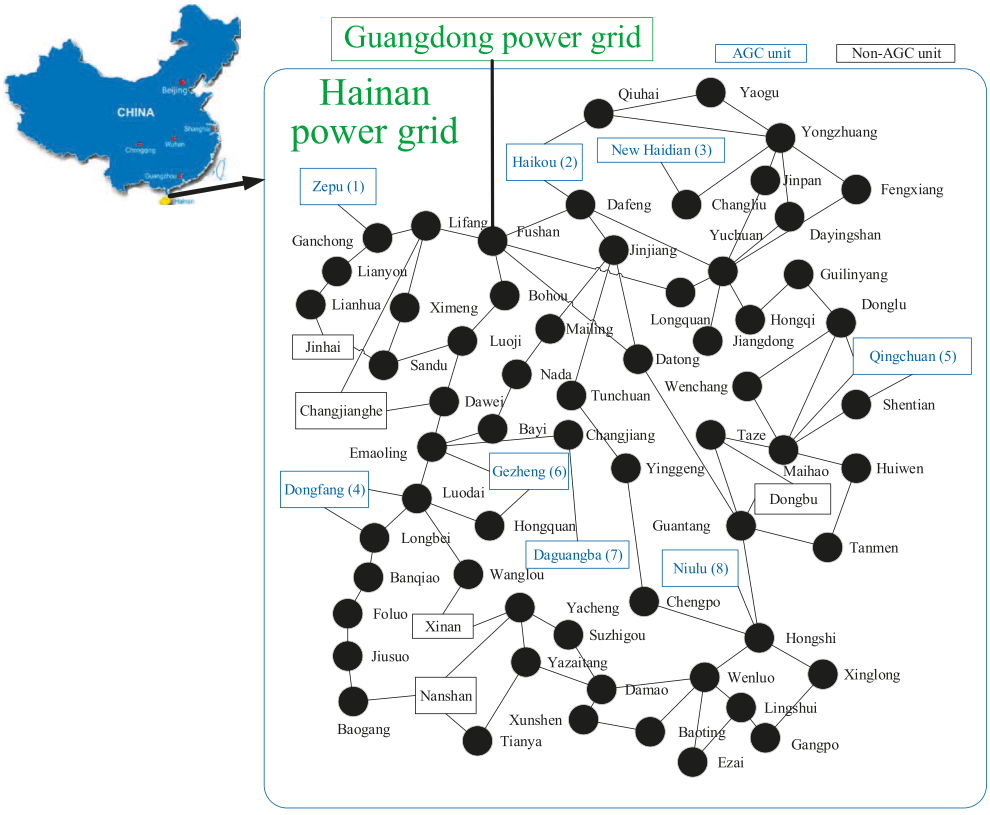

Fig. 8. Structure of Hainan power grid (2015).

Table 8
Statistic of simulation results (Hainan power gird, two objectives).

Algorithm	$\|\Delta f\|$(Hz)	ACE(MW)	Total cost($)	Tim.[a] (s)	Num.[b]
RDL	0.063423	164.0318	885,906,834.99	0.16071	2584
RANN	0.23939	570.6742	9,419,569,440.13	0.026026	85,003
UC + ED + AGC + GCD	0.26059	2110.2851	9,430,502,120.61	585.0315	15,728

[a] Tim. = Calculation time.
[b] Num. = Number of reverse regulations.

the next states of the power system, but also simultaneously provide multiple generation commands for all the AGC units in the power system; (iii) after the online training of the DNNs, the RDL based REG controller can online update the control policies for all the AGC units.

The major reasons that the optimal power flow of the ED is ignored are that: (i) Both generation control for active power and optimal power flow for reactive power are need to be considered in a complete power system. However, in general, the generation control and the optimal power flow are divided into two problems in the industry. Thus, this paper only considered the generation control problem. And since the divide of these two problems, the inputs and outputs of the generation controller can be reduced. Then, the training process of the proposed RDL can be reduced; (ii) The outputs of the generation controller based on the RDL meet the security constraint of node voltage; (iii) The designed framework of unified time scale can be applied to the optimal power flow for reactive power in a power system in the future.

As the statistic results of the case study of Hainan power grid shown (see Table 8 and Fig. 9), the RDL based REG controller can be employed in one area of a large-scale multi-area interconnected power system. Furthermore, compared Table 8 with Table 6, the gain in reducing the total operational cost of Hainan power grid is much less than that of IEEE New-England power system. Four major

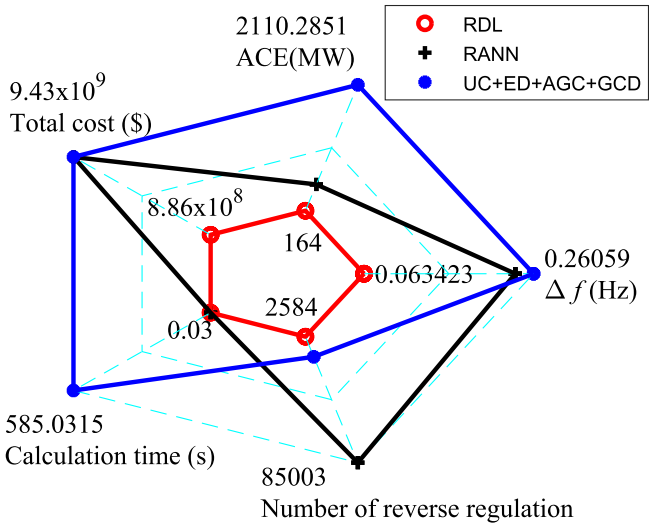

Fig. 9. Simulation results of Hainan power gird (frequency deviation, ACE, cost, calculation time, number of regulation).

reasons for the larger gain in reducing the total operational cost are that: (i) Some of AGC units programmed by the proposed RDL are shut-down while all the AGC units programmed by the conventional generation control are start-up at some time in the case of Hainan Power Grid; (ii) Some of AGC units programmed by both of the proposed RDL and the conventional generation control are shut-down at some time in the case of IEEE New-England power system; (iii) Since the DNNs of the RDL can learn the next states of the power system online, the number of the reverse regulations is reduced in the power system. Thus, the total operational cost obtained by the RDL based REG controller can be reduced; (iv) Since the DNNs of the RDL can learn the features of one area where the controller is utilized, the area control error of this area can be mitigated by the outputs of the controller of this area. Thus, the total operational cost obtained by this controller can be reduced once more.

Numerous DNN similar approaches can be combined with 'relaxed operator' as the REG controller, such as, artificial neural network in the paper, deep learning, etc. Parameters of these DNNs in RDL are tuned manually various times.

In the IEEE 118-bus power system, the RDL based REG controller

Table 9
Statistic of simulation results (Hainan power gird, three objectives).

Algorithm	$\|\Delta f\|$(Hz)	ACE(MW)	Total cost($)	Tim.[a] (s)	Num.[b]
RDL	0.078081	190.127	599,290,247.36	0.16381	2782
RANN	0.25443	796.0434	6,279,783,210.58	0.029494	118,332
UC + ED + AGC + GCD	0.23671	2185.1144	4,634,778,355.45	744.1344	19,520

[a] Tim. = Calculation time.
[b] Num. = Number of reverse regulations.

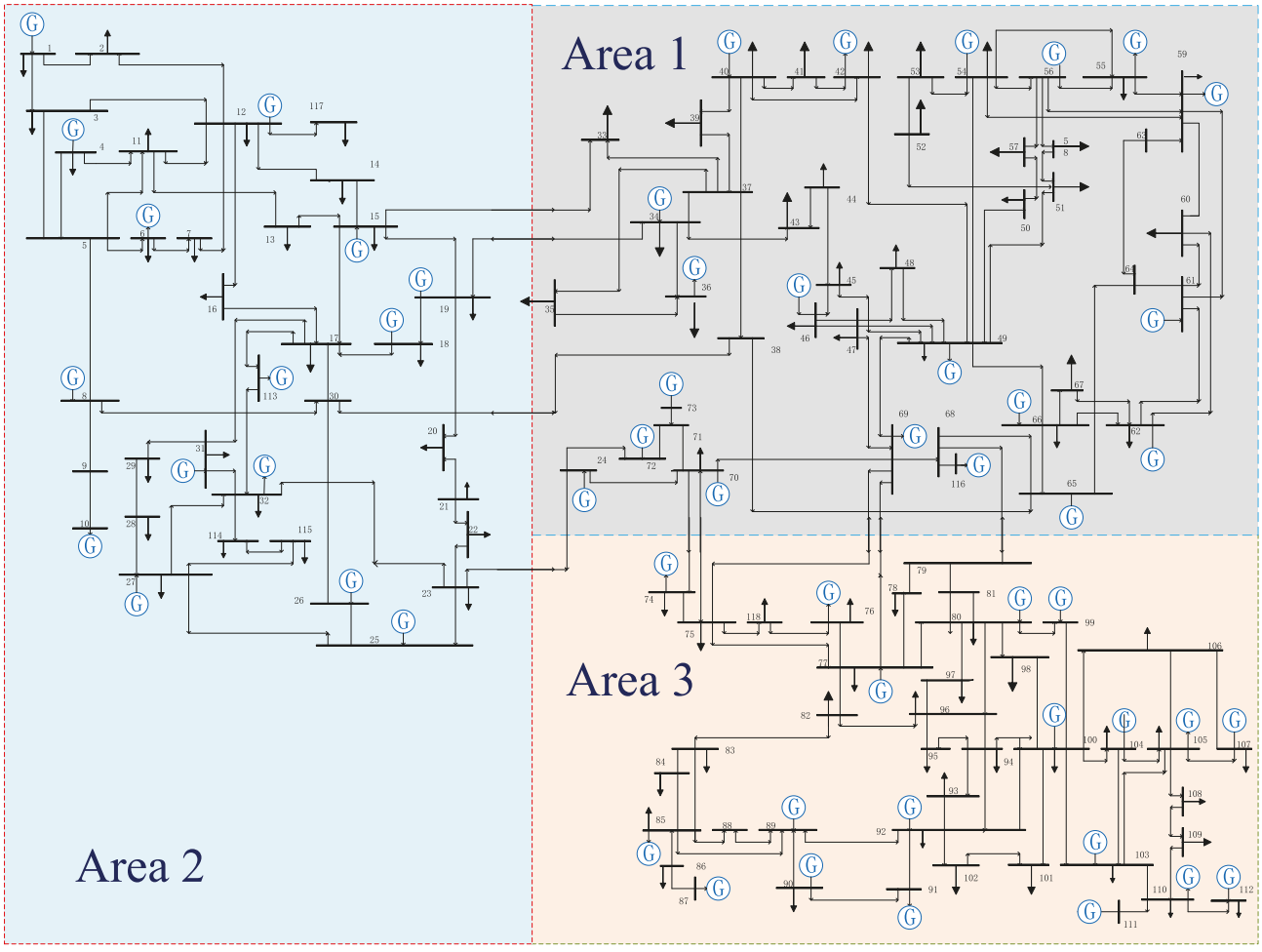

Fig. 10. Structure of the IEEE 118-bus power system.

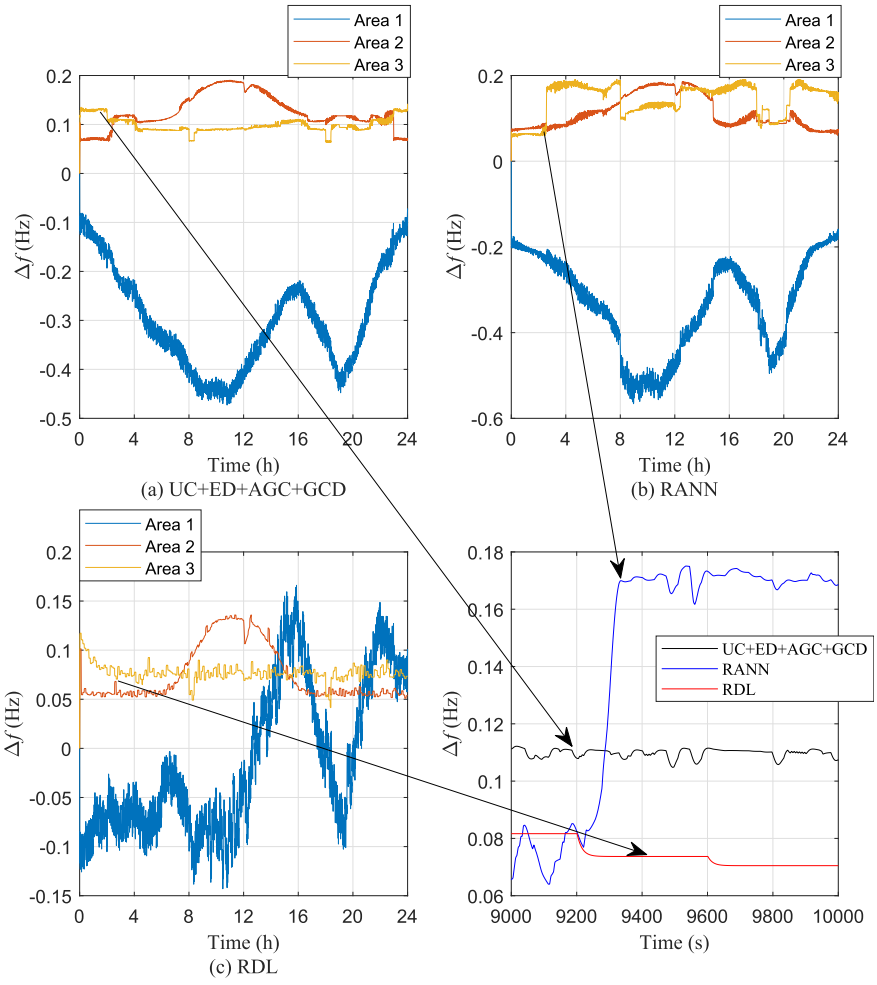

Fig. 11. Obtained frequency deviation of the IEEE 118-bus power system.

provides the most eligible generation commands for AGC units at the time from 9200 s to 9400 s compared with that of others algorithms. The major reason is that the designed DNN of the RDL can learn the features of a complex power system by its neural network structure.

To obtain better control performance of the REG controller, several difficulties should be overcame.

1. The REG controller could be ameliorated for the variable number of the outputs. The number of outputs in the REG controller should be increasing with the number of AGC units in the large-scale power system. Moreover, the RDL based REG controller should be re-pre-trained after the number of AGC units in the large-scale power system is changed.
2. The control performance of the RDL based REG controller is a data-hungry controller. The more accurate data means the better control performance. To obtain more accurate data for the REG controller, numerous artificial societies-computational experiments-parallel execution approaches can be employed into these simulations with graphics processing unit computing, such as parallel genetic algorithm [36].
3. The RDL based REG controller should be re-pre-trained when a power grid has flexible power nodes, which can be both generator and load at different cases, e.g., energy storage system, grid connected plug-in hybrid electric vehicles, etc.
4. Unfortunately, the start-up or shut-down states of units for power plants at the next day should be computed by the UC programming, which should be incompletely replaced by the RDL based REG controller in the case of that, the generator fuel of the power plant needs to be prepared in a short time, such as, just one day before.

6. Conclusions

To solve the collaboration problem of economic dispatch and generation control of multi-area power system, a REG framework is proposed in this paper, which towards an alternative to the conventional generation control framework. Then, RDL is proposed for the REG controller in this paper. The features of the RDL based REG controller can be summarized as,

(1) Compared with the conventional generation control framework, the REG framework is more compact one, and is a unified time scale framework.
(2) With the output ability of DNN, the RDL based REG controller can simultaneously provide multiple generation commands for AGC units in power system.
(3) With the learning ability of deep learning, RDL can effectively predict the next state of multi-area power system.
(4) The RDL based REG controller obtains the optimal control performance, meanwhile, the output actions can commit the constraints of the UC problem.

(5) The RDL based REG controller can be applied to solve the generation control and dispatch problem of multi-area power system.

Future work will mainly cover the development of the RDL algorithm for automatic voltage control or power system stability in a large-scale interconnected power system. Besides, two major limitations of the proposed RDL need to be handled in the future, i.e., (i) the pre-training time of the RDL could be significantly reduced by other more efficient training approaches; and (ii) the pre-training process of the RDL could be inherited automatically as the varying number of the controller outputs.

Acknowledgment

The authors gratefully acknowledge the support of the National Natural Science Foundation of China (NSFC) (51777078, 51477055).

Appendix A. Nomenclature

Variables

T	Number of time slots over the given period of time (h)
J_i	Number of generating units in the i-th area
$u_{j,t}$	State of the j-th generating unit at the t-th time slot
$u^*_{j,(1)}$	Temporary state of the j-th generating unit at the t-th time slot
$F_j(P_{j,t})$	Total fuel cost of the j-th generating unit (\$)
$SU_{j,t}$	Total start-up cost (\$)
$P_{j,t}$	Active power of the j-th generating unit at the t-th time slot (MW)
a_j	Constant factor of the generation cost
b_j	Linear factor of the generation cost
c_j	Quadratic factor of the generation cost
$T^{\mathrm{up}}_{j,t}$	Accumulate time slots of start-up state for the j-th generating unit at the t-th time slot (h)
$T^{\mathrm{down}}_{j,t}$	Accumulate time slots of shut-down state for the j-th generating unit at the t-th time slot (h)
$T^{\mathrm{min-down}}_j$	Minimized continuous shut-down time slot of the j-th generating unit (h)
T^{cold}_j	Time slots of the j-th generating unit for cold start-up (h)
$SU_{H,j}$	The j-th generating unit cost of heat start-up (t/(MW h))
$SU_{C,j}$	The j-th generating unit cost of cold start-up (t/(MW h))
$PD_{i,t}$	Total systemic load at the t-th time slot in the i-th area (MW)
P^{min}_j	Minimum and the maximum active power of the j-th generating unit in the i-th area (MW)
P^{max}_j	Maximum active power of the j-th generating unit in the i-th area (MW)
$SR_{i,t}$	Needed systemic spinning reserve at the t-th time slot in the i-th area (MW)
P^{up}_j	Maximum amplitude of the j-th generating unit for up-regulation (MW)
P^{down}_j	Maximum amplitude of the j-th generating unit for down-regulation (MW)
$T^{\mathrm{min-up}}_j$	Minimized continuous start-up time slot of the j-th generating unit (h)
$u_{j,(t-1)}$	State of the j-th generating unit at the $(t-1)$-th time slot
$F^{\mathrm{e}}_j(P_j)$	Generation cost of the j-th generating unit (\$)
P_j	Active power of the j-th generating unit (MW)
γ_j	Constant factor of the j-th generating unit for carbon emission
β_j	Linear factor of the j-th generating unit for carbon emission
α_j	Quadratic factor of the j-th generating unit for carbon emission
$F^{\mathrm{c}}_j(P_j)$	Carbon emission of the j-th generating unit (\$)
PD_i	Total systemic load in the i-th area (MW)
ω_{e}	Weight of economic objective for ED
ω_{c}	Weight of carbon emission reduction for ED
ω_{K}	Weight of network losses for ED
Δf_i	Frequency deviation of the i-th area (Hz)
e_i	Area control error of the i-th area (MW)
ΔP_i	Generation command for the i-th area (MW)
$P^{\mathrm{actual}}_{i,j}$	Actual generation command of the j-th AGC unit of the i-th area (MW)
t	Hour time slot of one day (h)
A	Actions set
$\Delta F'_{i,(t+1)}$	Prediction of next frequency deviation (Hz)
$u'_{j,t}$	Temporary start-up state
W_{mn}	Weight in the restricted Boltzmann machine
v_m	The m-th visible unit of DNN
v_m	The n-th hidden unit of DNN
φ_m	Offset of the m-th visible unit of DNN
μ_n	Offset of the n-th hidden unit of DNN
M	Number of visible units of each layer in DNN
N	Number of hidden units of each layer in DNN
p	Updated probability of action a
k_{p}	Probability coefficient

Abbreviations

REG	Real-time economic generation dispatch and control framework
DNN	Deep neural network
RDL	Relaxed deep learning
UC	Unit commitment
ED	Economic dispatch
AGC	Automatic generation control
GCD	Generation command dispatch
DRL	Deep reinforcement learning
RANN	Relaxed artificial neural network
ACE	Area control error
PID	Proportional-integral-differential
PV	Photovoltaic power
EV	Electric vehicle

Appendix B. Parameters of the conventional generation control algorithms

PID:proportional $k_{\mathrm{P}} = -0.006031543250198$, integral $k_{\mathrm{I}} = 0.00043250$;

Sliding mode controller:switch on/off point $k_{\mathrm{p}} = \pm 0.1$ Hz, output when on/off $k_{\mathrm{v}}\pm = 80$ (MW);

Active disturbance rejection control: extended state observer $A = \begin{bmatrix} 0 & 0.0001 & 0 & 0 \\ 0 & 0 & 0.0001 & 0 \\ 0 & 0 & 0 & 0.0001 \\ 0 & 0 & 0 & 0 \end{bmatrix}$, $B = \begin{bmatrix} 0 & 0 \\ 0 & 0 \\ 0.0001 & 0.0001 \\ 0 & 0 \end{bmatrix}$, $C = \mathrm{diag}(0.1 \quad 0.1 \quad 0.1 \quad 0.1)$, $D = \mathbf{0}_{4\times 2}$, $k_1 = 15.0$, $k_2 = 5.5$, $k_3 = 2.0$, $k_4 = 1$;

Fractional order PID: proportional $k_{\mathrm{P}} = -1$, integral

$k_I = 0.43250$, $\lambda = 1.3$, $\mu = 200$;

Fuzzy logic control: X (input, Δf) 21 grids from −0.2 to 0.2 (Hz), Y (input, $\int \Delta f$) 21 grids from −1 to 1 (Hz), Z (output, ΔP) is 441 grids from −150 to 150 (MW);

Q learning: actions set $A = \{-300, -240, -180, -120, -60, 0, 60, 120, 180, 240, 300\}$, learning rate $\alpha = 0.1$, the constant of probability distribution method $\beta = 0.5$, the discounted rate of future reward $\gamma = 0.9$;

Q(λ) learning: $A = \{-300, -240, -180, -120, -60, 0, 60, 120, 180, 240, 300\}$, $\alpha = 0.1$, $\beta = 0.5$, $\gamma = 0.9$, $\lambda = 0.9$;

R(λ) learning: $A = \{-300, -240, -180, -120, -60, 0, 60, 120, 180, 240, 300\}$, $\alpha = 0.1$, $\beta = 0.5$, $\gamma = 0.9$, $\lambda = 0.9$, $R_0 = 0$;

Genetic algorithm, simulated annealing arithmetic, multi-verse optimizer, grey wolf optimizer, particle swarm optimization of UC: the number of generations $N_g = 50$, population size $P_s = 10$;

Genetic algorithm, simulated annealing arithmetic, multi-verse optimizer, grey wolf optimizer, particle swarm optimization of ED: $N_g = 30$, $P_s = 10$;

Genetic algorithm, simulated annealing arithmetic, multi-verse optimizer, grey wolf optimizer, particle swarm optimization of GCD: $N_g = 5$, $P_s = 10$;

Fixed proportion: $k_j = \frac{\Delta P_j^{\max}}{\sum \Delta P_j^{\max}} \Delta P_j$, $j = 1, 2, \ldots, J_i$, i = 1, 2, …, 3.

References

[1] Jiang Q, Wang H. Two-time-scale coordination control for a battery energy storage system to mitigate wind power fluctuations. IEEE Trans Energy Convers 2013;28:52–61.
[2] Liang Z, Liang J, Zhang L, Wang C, Yun Z, Zhang X. Analysis of multi-scale chaotic characteristics of wind power based on hilbert-huang transform and hurst analysis. Appl Energy 2015;159:51–61.
[3] Chandra S, Gayme DF, Chakrabortty A. Time-scale modeling of wind-integrated power systems. IEEE Trans Power Syst 2016;31:4712–21.
[4] Wang B, Hobbs BF. Real-time markets for flexiramp: a stochastic unit commitment-based analysis. IEEE Trans Power Syst 2016;31:846–60.
[5] Hetzer J, Yu DC, Bhattarai K. An economic dispatch model incorporating wind power. IEEE Trans Energy Convers 2008;23:603–11.
[6] Battistelli C, Conejo A. Optimal management of the automatic generation control service in smart user grids including electric vehicles and distributed resources. Elec Power Syst Res 2014;111:22–31.
[7] Xi L, Zhang Z, Yang B, Huang L, Yu T. Wolf pack hunting strategy for automatic generation control of an islanding smart distribution network. Energy Convers Manag 2016;122:10–24.
[8] Zhang X, Yu T, Yang B, Li L. Virtual generation tribe based robust collaborative consensus algorithm for dynamic generation command dispatch optimization of smart grid. Energy 2016;101:34–51.
[9] Yu T, Wang YM, Ye WJ, Zhou B, Chan KW. Stochastic optimal generation command dispatch based on improved hierarchical reinforcement learning approach. IET Gener, Transm Distrib 2011;5:789–97.
[10] Li Z, Zang C, Zeng P, Yu H, Li S. Agent-based distributed and economic automatic generation control for droop-controlled ac microgrids. IET Gener, Transm Distrib 2016;10:3622–30.
[11] Li N, Zhao C, Chen L. Connecting automatic generation control and economic dispatch from an optimization view. IEEE Trans Control Netw Syst 2016;3:254–64.
[12] Botterud A, Zhou Z, Wang J, Sumaili J, Keko H, Mendes J, Bessa RJ, Miranda V. Demand dispatch and probabilistic wind power forecasting in unit commitment and economic dispatch: a case study of Illinois. IEEE Trans Sustain. Energy 2013;4:250–61.
[13] Li N, Zhao C, Chen L. Connecting automatic generation control and economic dispatch from an optimization view. IEEE Trans Control Netw Syst 2016;3:254–64.
[14] Silver D, Huang A, Maddison CJ, Guez A, Sifre L, Van Den Driessche G, Schrittwieser J, Antonoglou I, Panneershelvam V, Lanctot M, et al. Mastering the game of Go with deep neural networks and tree search. Nature 2016;529:484–9.
[15] Mnih V, Kavukcuoglu K, Silver D, Rusu AA, Veness J, Bellemare MG, Graves A, Riedmiller M, Fidjeland AK, Ostrovski G, et al. Human-level control through deep reinforcement learning. Nature 2015;518:529–33.
[16] Rahhal MA, Bazi Y, AlHichri H, Alajlan N, Melgani F, Yager R. Deep learning approach for active classification of electrocardiogram signals. Inf Sci 2016;345:340–54.
[17] Lecun Y, Bengio Y, Hinton G. Deep learning. Nature 2015;521:436–44.
[18] Kia M, Nazar MS, Sepasian MS, Heidari A, Siano P. Optimal day ahead scheduling of combined heat and power units with electrical and thermal storage considering security constraint of power system. Energy 2017;120:241–52.
[19] El-Hawary ME, Ravindranath KM. Combining loss and cost objectives in daily hydro-thermal economic scheduling. IEEE Trans Power Syst 1991;6:1106–12.
[20] Lin JC-W, Yang L, Fournier-Viger P, Wu JM-T, Hong T-P, Wang LS-L, Zhan J. Mining high-utility itemsets based on particle swarm optimization. Eng Appl Artif Intell 2016;55:320–30.
[21] Mantawy AH, Abdel-Magid YL, Selim SZ. Integrating genetic algorithms, tabu search, and simulated annealing for the unit commitment problem. IEEE Trans Power Syst 1999;14:829–36.
[22] Mirjalili S, Mirjalili SM, Hatamlou A. Multi-verse optimizer: a nature-inspired algorithm for global optimization. Neural Comput Appl 2016;27:495–513.
[23] Faris H, Aljarah I, Mirjalili S. Training feedforward neural networks using multi-verse optimizer for binary classification problems. Appl Intell 2016;45:1–11.
[24] Mirjalili S, Mirjalili SM, Lewis A. Grey wolf optimizer. Adv Eng Software 2014;69:46–61.
[25] Mirjalili S. How effective is the grey wolf optimizer in training multi-layer perceptrons. Appl Intell 2015;43:150–61.
[26] Yang B, Zhang XS, Yu T, Shu HC, Fang ZH. Grouped grey wolf optimizer for maximum power point tracking of DFIG based wind turbine. Energy Convers Manag 2017;133:427–43.
[27] Sahu RK, Panda S, Yegireddy NK. A novel hybrid deps optimized fuzzy PI/PID controller for load frequency control of multi-area interconnected power systems. J Process Contr 2014;24:1596–608.
[28] A robust PID controller based on imperialist competitive algorithm for load-frequency control of power systems. ISA Trans 2013;52:88–95.
[29] Dahiya P, Sharma V, Naresh R. Automatic generation control using disrupted oppositional based gravitational search spell optimised sliding mode controller under deregulated environment. IET Gener, Transm Distrib 2016;10:3995–4005.
[30] Liu F, Li Y, Cao Y, She J, Wu M. A two-layer active disturbance rejection controller design for load frequency control of interconnected power system. IEEE Trans Power Syst 2016;31:3320–1.
[31] Debbarma S, Saikia LC, Sinha N. Automatic generation control using two degree of freedom fractional order PID controller. Int J Electr Power Energy Syst 2014;58:120–9.
[32] Yu T, Zhou B, Chan KW, Lu E. Stochastic optimal CPS relaxed control methodology for interconnected power systems using Q-learning method. J Energy Eng 2010;137:116–29.
[33] Yu T, Zhou B, Chan KW, Chen L, Yang B. Stochastic optimal relaxed automatic generation control in non-markov environment based on multi-step Q(λ) learning. IEEE Trans Power Syst 2011;26:1272–82.
[34] Yu T, Wang H, Zhou B, Chan K, Tang J. Multi-agent correlated equilibrium Q(λ) learning for coordinated smart generation control of interconnected power grids. IEEE Trans Power Syst 2015;30:1669–79.
[35] Yu T, Zhou B, Chan K, Yuan Y, Yang B, Wu Q. R(λ) imitation learning for automatic generation control of interconnected power grids. Automatica 2012;48:2130–6.
[36] Wang K, Shen Z. A GPU-based parallel genetic algorithm for generating daily activity plans. IEEE Trans Intell Transport Syst 2012;13:1474–80.